The Astrophysical Journal, 700:L73–L77, 2009 August 1 doi:10.1088/0004-637X/700/2/L73

ON THE RELATIONSHIP BETWEEN DEBRIS DISKS AND PLANETS

Ágnes Kóspál[1], David R. Ardila[2], Attila Moór[3], and Péter Ábrahám[3]
[1] Leiden Observatory, Leiden University, P.O. Box 9513, 2300 RA, Leiden, The Netherlands; kospal@strw.leidenuniv.nl
[2] NASA Herschel Science Center, California Institute of Technology, Pasadena, CA 91125, USA
[3] Konkoly Observatory of the Hungarian Academy of Sciences, P.O. Box 67, 1525 Budapest, Hungary
Received 2009 March 27; accepted 2009 June 19; published 2009 July 10

ABSTRACT

Dust in debris disks is generated by collisions among planetesimals. The existence of these planetesimals is a consequence of the planet formation process, but the relationship between debris disks and planets has not been clearly established. Here we analyze *Spitzer*/MIPS 24 and 70 μm data for 150 planet-bearing stars, and compare the incidence of debris disks around these stars with a sample of 118 stars around which planets have been searched for, but not found. Together they comprise the largest sample ever assembled to deal with this question. The use of survival analysis techniques allows us to account for the large number of nondetections at 70 μm. We discovered 10 new debris disks around stars with planets and one around a star without known planets. We found that the incidence of debris disks is marginally higher among stars with planets, than among those without, and that the brightness of the average debris disk is not significantly different in the two samples. We conclude that the presence of a planet that has been detected via current radial velocity techniques is not a good predictor of the presence of a debris disk detected at infrared wavelengths.

Key words: circumstellar matter – infrared: stars – Kuiper Belt – planetary systems

Online-only material: machine-readable table

1. INTRODUCTION

As of the end of 2008, 228 extrasolar planets around 193 stars had been discovered using radial velocity techniques. Most of them are believed to be Jupiter-like gas giants, although some may be lower-mass rocky planets (Udry & Santos 2007). According to the core accretion model, planets are formed by the agglomeration of rocky planetesimals into solid cores (Lissauer 2005). For gas giants, the core accretes a gaseous envelope. The planets may migrate toward the star due to interactions with the disk material (Lin et al. 2000), and strong planet–planet gravitational scattering may significantly modify orbital parameters (Raymond et al. 2008).

It is also known that many main-sequence stars display infrared and/or submillimeter excess emission due to the presence of debris dust grains (e.g., Trilling et al. 2008). These grains are replenished by collisions among planetesimals, leftovers of the planet formation process (Backman & Paresce 1993). Planets orbiting the star can stir the planetesimal population and initiate a collisional cascade, resulting in dust production. The morphology of the disk might be gravitationally shaped by planets orbiting interior to the disk (Chiang et al. 2009). The common origin of planets and debris disks suggests that a connection may exist between the presence of planets and planetesimals.

The relationship between debris disks and planets can be studied by comparing the incidence of excess emission due to debris dust between samples of stars with and without planets. An overview of such studies is presented in Table 1. For Sun-like stars, e.g., Beichman et al. (2005, 2006) hinted at a positive correlation between debris disks and planets; Moro-Martín et al. (2007) found no significant correlation; and Trilling et al. (2008) claimed that although excess rates for the planet sample are higher, both samples' excess rates are consistent at the 1σ level. More conclusive results can only be based on larger samples than used in those studies.

Here we use data from the *Spitzer Space Telescope* archive at 24 and 70 μm to compare the incidence of debris dust around stars with planets (SWPs) discovered/confirmed using radial velocity techniques and those where radial velocity measurements did not indicate planetary companions (stars without planets, SWOPs). We use all public data constructing the largest sample ever considered in attacking this question.

2. OBSERVATIONS

2.1. Sample Selection

We considered 193 SWPs discovered/confirmed using radial velocity measurements as of 2008 December.[4] Out of these, 150 have publicly available *Spitzer*/MIPS 24 and/or 70 μm measurements (all of them were observed at 70 μm, 83 of them at 24 μm). These constitute our planet-bearing sample. For SWOPs, we used those stars that were present in the Keck, Lick, and Anglo-Australian Telescope planet search programs (Wright et al. 2004; Valenti & Fischer 2005), but around which no planets were found. These stars have no planets with radial velocity semi-amplitudes $K > 30\,\mathrm{m\ s^{-1}}$ and orbital periods shorter than four years, and the radial velocity measurements have a typical Doppler precision of 3 m s^{-1}. We based our SWOPs sample on two *Spitzer* surveys of nearby stars (Pid 41 and Pid 2324) and discarded some stars where close-by objects would have contaminated the MIPS photometry. The resulting SWOPs sample includes 118 objects (all of them were observed at 24 μm, all but one at 70 μm, see Table 2). Both samples contain stars with spectral types between F3 and M3. While the majority are main-sequence stars, a few subgiants are also present, and the SWPs sample also contains four giants. As age is a key parameter in debris disk evolution (Wyatt 2008), we checked whether the ages differed significantly in the two samples. We calculated two-sample tests (Gehan's generalized Wilcoxon test, logrank test, Peto & Peto generalized Wilcoxon test, and Peto & Prentice generalized Wilcoxon test), and found

[4] Regularly updated lists of extrasolar planets can be found at http://www.exoplanets.org and at http://www.exoplanet.eu.

Table 1
Spitzer-Based Surveys of Debris Disks Around Main-Sequence Stars (Stars with Excess/Total Observed Sample)

Reference	Sample	24 μm		70 μm	
		SWP	SWOP	SWP	SWOP
Beichman et al. (2005)	FGK	0/25 (0%)	...	6/25 (24%)	...
Bryden et al. (2006)	FGK	1/12 (8%)	0/57 (0%)	1/12 (8%)	6/57 (10%)
Beichman et al. (2006)	FGKM	...	5/88 (6%)	...	12/88 (14%)
Su et al. (2006)	A	...	50/155 (32%)	...	44/134 (33%)
Gautier et al. (2007)	M	0/3 (0%)	0/59 (0%)	0/3 (0%)	0/38 (0%)
Moro-Martín et al. (2007)	FGK	0/9 (0%)	2/99 (2%)	1/9 (11%)	9/99 (9%)
Trilling et al. (2008)	FGK	3/45 (7%)	4/139 (3%)	10/48 (21%)	22/148 (15%)
Carpenter et al. (2009)	FGK	0/10 (0%)	41/299 (14%)	2/10 (20%)	19/299 (6%)
present work	**FGKM**	**3/83 (4%)**	**1/118 (1%)**	**22/150 (15%)**	**17/117 (15%)**

Table 2
Photospheric Predictions and MIPS Photometry

Name	Type	Age (Gyr)	Age ref	[Fe/H]	$F_{24}^{\rm pred}$ (mJy)	$F_{24}^{\rm obs}$ (mJy)	σ_{24} (mJy)	R_{24}	χ_{24}	IRE$_{24}$[a]	$F_{70}^{\rm pred}$ (mJy)	$F_{70}^{\rm obs}$ (mJy)	σ_{70} (mJy)	R_{70}	χ_{70}	IRE$_{70}$[b]
HD 142	SWP	3.120	1	0.0875	109.5	119.6	4.90	1.09	2.06	NO	11.92	18.16	2.73	1.52	2.28	NO
HD 166	SWOP	0.200	2	−0.0600	134.6	157.4	6.45	1.17	3.53	YES	14.68	102.9	8.42	7.01	10.48	YES
HD 1237	SWP	0.625	3	0.1100	79.40	82.61	3.39	1.04	0.95	NO	8.67	11.07	1.68	1.28	1.43	NO
HD 1581	SWOP	4.840	1	−0.2025	567.6	527.1	21.61	0.93	−1.87	NO	62.13	74.40	7.93	1.20	1.55	NO
HD 3651	SWP	8.200	4	−0.0540	187.8	188.2	7.72	1.00	0.05	NO	20.51	15.49	5.12	0.76	−0.98	NO
HD 3823	SWOP	7.200	1	−0.3100	110.8	111.8	4.58	0.01	0.20	NO	12.14	<13.49	...	<1.11	...	UPL
HD 3795	SWOP	11.600	1	−0.6425	130.0	135.7	5.56	1.04	1.03	NO	14.30	13.92	2.49	0.97	−0.15	NO
HD 4208	SWP	7.760	1	−0.2600	24.81	...	...	...	...	...	2.72	<5.35	...	<1.96	...	UPL
HD 4308	SWP	8.680	1	−0.3933	73.67	74.73	3.06	1.01	0.35	NO	8.08	<13.00	...	<1.61	...	UPL

Notes.
[a] Infrared excess at 24 μm. SWPs with excess: HD 10647, HD 22049, HD 69830. SWOPs with excess: HD 166.
[b] Infrared excess at 70 μm. SWPs with excess: GJ 581, HD 10647, HD 19994, HD 22049, HD 33636, HD 38529, HD 40979, HD 46375, HD 50499, HD 50554, HD 52265, HD 69830, HD 73526, HD 82943, HD 117176, HD 128311, HD 137759, HD 178911, HD 187085, HD 192263, HD 202206, HD 216435. SWOPs with excess: HD 166, HD 7570, HD 17925, HD 20794, HD 20807, HD 22484, HD 30495, HD 38858, HD 43162, HD 48682, HD 72905, HD 76151, HD 115617, HD 118972, HD 158633, HD 206860, HD 207129.

(This table is available in its entirety in a machine-readable form in the online journal. A portion is shown here for guidance regarding its form and content.)

that the age distributions do not differ (mean ages are 5.317 Gyr for SWPs and 4.648 Gyr for SWOPs). The same holds for the effective temperatures (mean effective temperatures are 5460 K for SWPs and 5550 K for SWOPs).

2.2. Data Processing

2.2.1. Data Reduction

From the *Spitzer* archive we downloaded BCD files reduced with the SSC pipeline version 16.0 or 16.1. At 70 μm, we used GeRT (version S14.0 v1.1 [060415]) to do column mean subtraction and time filtering on the BCD files. We used Mopex (version 18.1.5) to create mosaics for 24 and 70 μm images and obtained aperture photometry using IDL. At 24 μm, we used an aperture radius of 7″, sky annulus between 40″ and 50″, and aperture correction of 1.61; at 70 μm, we used an aperture radius of 8″, sky annulus between 39″ and 65″, and aperture correction of 3.70, appropriate for a 10,000 K blackbody. After identifying stars with 70 μm excess, we recalculated their fluxes with an aperture correction of 3.83, appropriate for a 60 K blackbody. Appropriate color corrections were also performed. Thanks to the small aperture, nearby sources had no effect on our photometry. At 24 μm, the aperture was placed around the centroid of each star, while at 70 μm, the aperture was placed at the same position as for the 24 μm image. If a 24 μm position was not available, we used fixed coordinates. For sources brighter than 100 mJy and having signal-to-noise ratio of $\geqslant$11, we checked their spatial extent by comparing the images to a stellar point-spread function (PSF). For extended objects (HD 10647, HD 38858, HD 207129, HD 48682, and HD 115617) photometry was extracted by fitting a PSF broadened by an appropriate two-dimensional Gaussian. The fluxes of ϵ Eri were taken from Backman et al. (2009).

2.2.2. Photosphere Prediction

We collected near-infrared photometry from the 2MASS All-Sky Catalog of Point Sources (Skrutskie et al. 2006), Morel & Magnenat (1978), and Ducati (2002), 8.28 μm fluxes from the MSX Infrared Point-Source Catalog (Egan et al. 2003), and 12 μm fluxes from the IRAS catalog of point sources (with appropriate color correction). Spectral types, effective temperatures, and metallicities came from the NASA Star and Exoplanet Database.[5] For each FGK star we selected the model from the ATLAS9 grid of model atmospheres (Castelli & Kurucz 2003) that has the closest metallicity, $\log g = 4.5$, and interpolated between the two closest models in effective temperature. This model spectrum was then scaled to the near- and mid-infrared photometric points, and its value at 23.68 μm and at 71.42 μm was calculated. M stars were similarly fitted with NextGen model atmospheres (Hauschildt et al. 1999). The resulting photospheric fluxes ($F_{24}^{\rm pred}$, $F_{70}^{\rm pred}$) are presented in Table 2.

[5] http://nsted.ipac.caltech.edu/

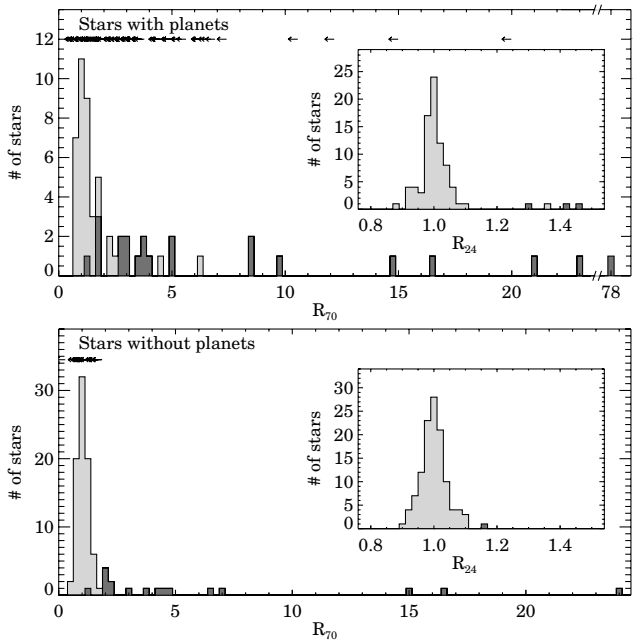

Figure 1. Distribution of observed-to-predicted flux ratios at 70 and 24 μm (R_{70} in the big graphs, and R_{24} in the small insets). Stars with significant ($>3\sigma$) excess are indicated with dark shades. Upper limits are indicated with left arrows.

2.2.3. Empirical Correction

To test our photometric predictions, we considered the ratio of the observed and predicted flux (R_{24}, R_{70}) as a function of the logarithm of the observed brightness ($\log(F_{24}^{\rm obs})$, $\log(F_{70}^{\rm obs})$). We found that $F_{24}^{\rm obs}$ tends to be systematically higher than $F_{24}^{\rm pred}$ for bright stars. At 70 μm no such trend could be seen. At 24 μm the points could be well fitted with a linear relationship, which we used to correct the observed fluxes (note that Gordon et al. 2007 found a similar dependence of the 70 μm aperture photometry on source brightness, see their Figures 3 and 4). The correction was always less than 6%. We found no dependence of the corrected flux on the effective temperature. This is in agreement with Engelbracht et al. (2007), though is in contrast with Beichman et al. (2006). Our *Spitzer*/MIPS 24 and 70 μm photometry, together with individual uncertainties (including those of the absolute flux calibration of the MIPS instrument, 4% at 24 and 7% at 70 μm; see the MIPS Data Handbook) can be seen in Table 2.

3. RESULTS

3.1. Identification of Debris Disks

In all 24 μm observations the target was detected at $>3\sigma$ level, where σ is the flux uncertainty. At 70 μm, 59 out of 150 SWPs, and 97 out of 117 SWOPs were detected at $>3\sigma$ level. For the nondetections at 70 μm, upper limits were calculated as $3\sigma_{70}$ if the observed flux in the aperture ($F_{70}^{\rm obs}$) was negative, and $F_{70}^{\rm obs} + 3\sigma_{70}$ if positive (Carpenter et al. 2009). A star has significant excess if $\chi_{70} = (F_{70}^{\rm obs} - F_{70}^{\rm pred})/\sigma_{70} > 3$ (Table 2). In the SWPs sample, three stars have significant excess at 24 μm, and 22 stars at 70 μm. In the SWOPs sample, one star shows significant 24 μm excess, while 17 stars have significant excess at 70 μm. The names of stars with excess are listed in the notes to Table 2.

Figure 1 shows the histogram of observed-to-photospheric flux ratios at 24 and 70 μm (R_{24}, R_{70}). At both wavelengths the distribution peaks at $R \approx 1$, and can be approximated with a Gaussian of $\sigma = 4\%$ at 24 μm (the error budget is dominated by the uncertainty of the absolute flux calibration) and $\sigma = 24\%$ at 70 μm (the photometry is confusion noise limited at this wavelength). Out of the 39 stars with excess, shown with dark shades in Figure 1, 28 were known in the literature to harbor debris disks. For the remaining 11 our work shows the first indication for a debris disk (Table 3).

Table 3
Newly Identified Debris Disks

Name	$F_{70}^{\rm pred}$ (mJy)	$F_{70}^{\rm obs}$ (mJy)	σ_{70} (mJy)	R_{70}	χ_{70}	$L_{\rm dust}/L_*$
GJ 581[a]	5.98	16.47	2.94	2.753	3.567	1.2×10^{-5}
HD 40979[a]	5.11	14.24	2.73	2.784	3.346	1.2×10^{-5}
HD 43162[b]	10.01	19.82	2.95	1.980	3.329	1.0×10^{-5}
HD 46375[a]	3.23	74.68	19.04	23.102	3.753	2.3×10^{-4}
HD 50499[a]	3.62	10.70	2.16	2.957	3.273	1.3×10^{-5}
HD 73526[a]	0.91	19.11	5.38	20.943	3.382	1.7×10^{-4}
HD 137759[a]	455.52	615.53	44.08	1.351	3.630	4.3×10^{-6}
HD 178911[a]	2.23	11.43	1.88	5.119	4.891	3.6×10^{-5}
HD 187085[a]	3.45	13.34	2.81	3.867	3.520	1.8×10^{-5}
HD 202206[a]	2.00	29.51	3.77	14.735	7.290	1.1×10^{-4}
HD 216435[a]	10.88	41.74	4.04	3.836	7.636	2.0×10^{-5}

Notes.
[a] Stars with planets.
[b] Stars without planets.

3.2 Survival Analysis

At 24 μm, all observed stars were detected at several σ level. Thus, the distribution of excesses can be compared with traditional two-sample tests, which show that SWPs and SWOPs do not differ. This is due to the fact that the overwhelming majority of stars exhibit pure photospheric emission at 24 μm.

The 70 μm data set is censored—there are upper limits—and survival analysis is required to compare the two distributions (e.g., Moro-Martín et al. 2007). The Kaplan–Meier (KM) estimator gives the cumulative distribution of a statistical variable taking into account the upper limits (e.g., Feigelson & Nelson 1985). To use survival analysis, the censoring should not depend on the variable itself. This condition can be fulfilled by using the observed-to-photospheric flux ratio (R_{24} and R_{70}) as the variable. In average SWPs are farther than SWOPs. As a consequence, the former tend to be apparently fainter than the latter, resulting in more nondetections in the SWPs sample, introducing Malmquist bias. This bias is eliminated by using the distance-independent observed-to-photospheric flux ratio.

Figure 2 presents the KM estimators for our SWPs and SWOPs samples. Calculations were done with the ASURV Rev. 1.2 package (Lavalley et al. 1992), which implements the methods presented in Feigelson & Nelson (1985). As with the two-sample tests, the KM estimators show that at 24 μm there is no difference between the distribution of excesses of SWPs and of SWOPs. At 70 μm, however, the two KM curves are marginally different. The largest distance between the curves occurs at $R_{70} = 1.5$. The values at this point are 0.273 ± 0.045 and 0.155 ± 0.034 for SWPs and SWOPs, respectively, a 2.1σ difference. Thus, SWPs tend to have excesses slightly more often than SWOPs. Other statistical tests also suggest that the distributions are marginally different. For example, Gehan's generalized Wilcoxon test indicates that the probability of the null hypothesis—that SWPs and SWOPs have the same incidence of debris disks—is 13%. Other tests give probabilities

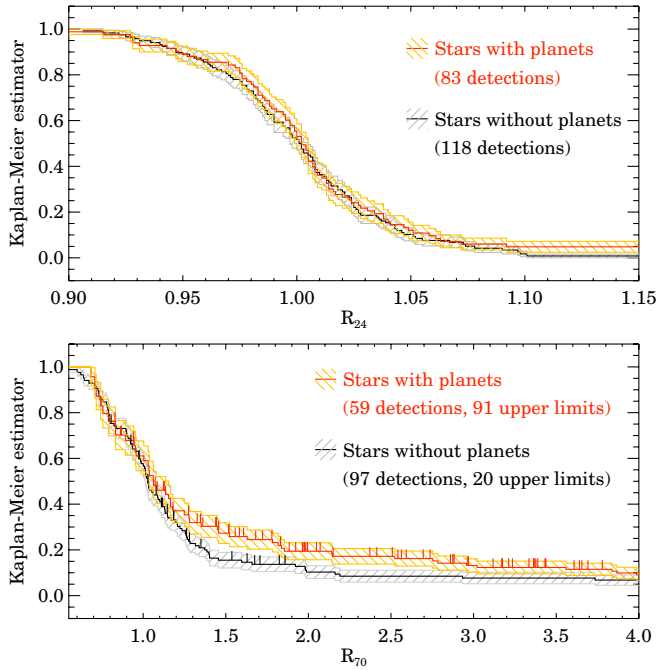

Figure 2. KM estimators for our two samples as a function of observed-to-photospheric flux ratio at 24 μm (upper panel) and at 70 μm (lower panel). Upper limits are indicated by vertical dashes. The KM estimator at a certain flux ratio gives the fraction of stars having a flux ratio larger than that value.

between 20% and 40%. To increase the significance of the obtained 2.1σ difference to 5σ would require about five times more objects in each sample. The mean excess at 70 μm, as given by the area under the KM estimator curves is 2.975 $\pm$ 0.732 for SWPs, and 1.725 $\pm$ 0.273 for SWOPs. Though disks around SWPs tend to be brighter, the difference is only 1.6σ. The results do not change significantly if we discard the four giant stars from the SWPs sample.

The common way in the literature to calculate detection rates is to divide the number of stars with excess by the number of all observed stars (Table 1). At 70 μm this method gives a detection rate of 15% for both SWPs and SWOPs. However, if we were to divide by the number of detected sources only, we would conclude that 37% of the SWPs have excesses, compared to 18% of the SWOP sample. The discrepancy of these methods is related to the presence of upper limits, which are correctly handled in our survival analysis.

4. DISCUSSION

It is an open question whether the orbital parameters of the planets correlate with the presence of debris disks (Chiang et al. 2009). We compared stars with and without excesses within the SWP sample. The two-sample tests mentioned above show that the planets' semimajor axes follow the same distribution in the two groups, while eccentricities and masses are slightly higher for stars having both planets and debris disks than those without debris disks, although the differences are not statistically significant.

The mean metallicities for our stars are [Fe/H] = 0.103 $\pm$ 0.018 and $-$0.097 $\pm$ 0.024 for SWPs and SWOPs, respectively. As expected (Santos et al. 2001; Valenti & Fischer 2005), two-sample tests show the metallicity distributions to be significantly different in our samples. To check whether there are differences in the distribution of excesses between metal-rich and metal-poor stars, we analyzed the SWPs and SWOPs samples separately. For each sample, we compared R_{70} between the bottom and top thirds of the metallicity distributions, using KM estimators. We found that metallicity does not correlate with the infrared excess in either sample, confirming results obtained for smaller samples (Greaves et al. 2006; Beichman et al. 2005; Bryden et al. 2006). While metallicity is one of the strongest predictors for the presence of giant planets (Valenti & Fischer 2005), it does not predict the presence of debris disks.

Moro-Martín et al. (2007) argued that the larger metallicity of SWPs implies that more planetesimals were formed early in those systems but that most were expelled due to the orbital evolution of the giant planets. The planetesimal configuration is then the same that would occur in an average metallicity SWOPs. This implies that debris disks are more common around metal-rich stars without planets, which is in contrast to the observations presented here.

Around a 1 $L_\odot$ solar-type star, a narrow ring of dust particles radiating as blackbodies would have the peak of its emission (F_ν) at 24 μm if located at 1.7 AU from the star. The gravitational influence of giant planets extends at most to the 3:1 mean motion resonance (e.g., Moro-Martín & Malhotra 2005). For our sample, where the average semimajor axis is 1.4 AU, this would be 2.9 AU. Thus, these planets might stir the planetesimals located within a belt similar to the asteroid belt in our solar system. However, our results show that 24 μm excess is rare in both SWPs and SWOPs. Moreover, not all stars exhibiting 24 μm excess have dust within this region: the warmest dust present in these systems is 60 K dust at a radius of 25 AU for HD 10647 (Liseau et al. 2008), 120 K dust at 3 AU for HD 22049 (Backman et al. 2009), 245 K dust at 1 AU for HD 69830 (Lisse et al. 2007), and 87 K dust at 9.1 AU for HD 166 (Trilling et al. 2008). This implies that warm debris dust is intrinsically rare in both SWPs and SWOPs, thus the physical reason of this rarity is probably unrelated to the planets. With so few stars with 24 μm excess, the KM estimators cannot rule out any difference between the SWPs and the SWOPs samples. Our observations do not preclude that there are differences between the two samples in the distribution of asteroid belt-type debris disks fainter than our detection limit at 24 μm ($L_{\rm dust}/L_* \approx 10^{-5}$, as calculated from Equation (11) of Wyatt 2008).

Debris dust peaking at 70 μm is usually too far from the planets considered here to be affected by their presence. Dust distances for debris disk systems with excesses at 70 μm are mostly larger than 4–5 AU (Trilling et al. 2008). The null hypothesis is consistent with that measurement. Trilling et al. (2008) argued that stars with planets are typically farther and in more confused regions of the sky, and suggest that dust around them may be more common than what detections indicate. In our sample, the median distance to the SWPs is 35 pc, compared to the 15 pc for the SWOPs, and two-sample tests reveal these distances to be significantly different. However, our main analysis quantity is the distance-independent R, and we explicitly include information about sky confusion noise in the form of upper limits, which are taken into account in the survival analysis. Therefore, our results do not support the presence of a large population of undiscovered debris disks around SWPs.

At 70 μm, our detection limit (Equation (11) of Wyatt 2008) is $L_{\rm dust}/L_* \approx 10^{-6}$. For these bright debris disks, the null hypothesis implies that the population of planets at distances where the 70 μm emission comes from is the same for SWPs and the SWOPs. The marginally higher incidence of debris disks around SWPs suggests that in these systems an outer planet

might also exist, which stirs up the planetesimals producing a cold debris disk.

The model by Wyatt et al. (2007) for A-type stars suggests that the 70 μm emission should be larger for SWPs than for SWOPs, due to the larger mass of the protoplanetary disk in the former. They speculate that a similar trend holds for Sun-like stars. We found that the brightest debris disks in our SWPs sample are 2–3 times brighter than those in the SWOPs sample, but the mean brightnesses are only slightly higher in the SWPs sample at a 1.6σ level. Our results do not contradict with the prediction of Wyatt et al. (2007), although the difference we found is less pronounced than that expected for A-type stars. Note that disk mass is not the only variable that controls the likelihood of planet formation: disk lifetime, metallicity, and surface density distribution are also important.

5. SUMMARY AND CONCLUSIONS

Prior to this study, only a dozen stars were known to harbor both planets and debris disks. Our 10 new debris disks found around planet-bearing stars at 70 μm doubled this number. We analyze a sample of planet-host stars at least three times larger than any previous studies and a carefully chosen control sample of stars without planets that is comparable in size. We have found that the incidence of debris disks (measured at 70 μm) is only marginally higher among stars with planets, than among those without. This result suggests the possibility that—if debris production is primarily due to stirring by planets—the planet population at large radii (larger than what current radial velocity surveys can find) is comparable in both samples (although there are other possibilities for debris production, such as planetesimal self-stirring, or external perturbations). We found that the brightness of the average debris disk is not significantly different in the two samples. We could not discover any clear correlation between the planets' orbital parameters or the parent stars' metallicity and the presence of debris dust.

This work is based on observations made with the *Spitzer Space Telescope*, which is operated by the Jet Propulsion Laboratory, California Institute of Technology under a contract with NASA. Á.K. acknowledges support from the *Spitzer* Visiting Graduate Student Fellowship and from the Netherlands Organization for Scientific Research (NWO). The authors thank L. Balázs for useful discussions about statistics and the referee for his/her comments. This work was partly supported by the Hungarian Research Fund OTKA K62304.

Facilities: Spitzer

REFERENCES

Backman, D., & Paresce, F. 1993, Protostars and Planets III, ed. E. H. Levy & J. I. Lunine (Tucson, AZ: Univ. Arizona Press), 1253
Backman, D., et al. 2009, ApJ, 690, 1522
Beichman, C. A., et al. 2005, ApJ, 622, 1160
Beichman, C. A., et al. 2006, ApJ, 652, 1674
Bryden, G., et al. 2006, ApJ, 636, 1098
Carpenter, J. M., et al. 2009, ApJS, 181, 197
Castelli, F., & Kurucz, R. L. 2003, in Proc. IAU Symp. 210, Modelling of Stellar Atmospheres, ed. N. Piskunov, W. W. Weiss, & D. F. Gray (Dordrecht: Kluwer), 20
Chiang, E., Kite, E., Kalas, P., Graham, J. R., & Clampin, M. 2009, ApJ, 693, 734
Ducati, J. R. 2002, VizieR Online Data Catalog, 2237 (http://cdsads.u~strasbg.fr/abs/2002yCat.2237....OD)
Egan, M. P., et al. 2003, Air Force Research Laboratory Technical Report AFRL-VS-TR-2003-1589
Engelbracht, C. W., et al. 2007, PASP, 119, 994
Feigelson, E. D., & Nelson, P. I. 1985, ApJ, 293, 192
Gautier, Th. N., et al. 2007, ApJ, 667, 527
Gordon, K. D., et al. 2007, PASP, 119, 1019
Greaves, J. S., Fischer, D. A., & Wyatt, M. C. 2006, MNRAS, 366, 283
Hauschildt, P. H., Allard, F., & Baron, E. 1999, ApJ, 512, 377
Lavalley, M., Isobe, T., & Feigelson, E. 1992, in ASP Conf. Ser. 25, Astronomical Data Analysis Software and Systems I, ed. D. M. Worrall, C. Biemesderfer, & J. Barnes (San Francisco, CA: ASP), 245
Lin, D. N. C., Papaloizou, J. C. B., Terquem, C., Bryden, G., & Ida, S. 2000, in Protostars and Planets IV, ed. V. Mannings, A. P. Boss, & S. S. Russell (Tucson, AZ: Univ. Arizona Press), 1111
Liseau, R., et al. 2008, A&A, 480, L47
Lissauer, J. J. 2005, Space Sci. Rev., 116, 11
Lisse, C. M., Beichman, C. A., Bryden, G., & Wyatt, M. C. 2007, ApJ, 658, 584
Morel, M., & Magnenat, P. 1978, A&AS, 34, 477
Moro-Martín, A., & Malhotra, R. 2005, ApJ, 633, 1150
Moro-Martín, A., et al. 2007, ApJ, 658, 1312
Raymond, S. N., Barnes, R., Armitage, P. J., & Gorelick, N. 2008, ApJ, 687, L107
Santos, N. C., Israelian, G., & Mayor, M. 2001, A&A, 373, 1019
Skrutskie, M. F., et al. 2006, AJ, 131, 1163
Su, K. Y. L., et al. 2006, ApJ, 653, 675
Trilling, D. E., et al. 2008, ApJ, 674, 1086
Udry, S., & Santos, N. C. 2007, ARA&A, 45, 397
Valenti, J. A., & Fischer, D. A. 2005, ApJS, 159, 141
Wright, J. T., Marcy, G. W., Butler, R. P., & Vogt, S. S. 2004, ApJS, 152, 261
Wyatt, M. C. 2008, ARA&A, 46, 339
Wyatt, M. C., Clarke, C. J., & Greaves, J. S. 2007, MNRAS, 380, 1737